Chapter 7

7.1 Comparison and Conclusion

Oxides of transition and rare earth elements have been reported to have excellent optical properties. This work is an attempt to investigate the luminescent properties of some oxides with rare earth activators. The Oxides were synthesized by several methods.

Rare earth oxides of Cerium and Lanthanum were selected for study as they can be cost effective luminescent materials. Zirconium oxide has excellent potential as a luminescent host material and hence it was also selected for study. These oxides were activated with the rare earth ions of Europium and Terbium, which are known for their emission properties.

The aim was to synthesize these oxides by the quick and easy combustion assisted heating. These methods provide oxides in nanocrystalline form. For the sake of reference, one bulk sample was also prepared by solid state method while another nano particulate sample was prepared by co – precipitation. All these synthesis techniques are relative simple, quick and easy. For comparison of bulk properties, commercially available material was also procured.

In this chapter, comparison has been made between the synthesized materials and between the techniques of synthesis in terms of structural aspects and optical characteristics.

The combustion synthesis of Ceria resulted in sudden outburst of energy without much flame, while in case of Zirconia, the reaction persisted for relatively longer time with white flame. Synthesis of Lanthanum oxide was more in line with Zirconia, giving an orangish flame for a shorter duration.

Samples synthesized by solid state method show better crystallinity compared to those prepared by Co – precipitation method. The XRD peak intensities of combustion made samples do not show any specific pattern of variation. This is on expected lines as there are several synthesis parameters involved leading to a degree of inconsistency, which is perhaps inherent in the process. However, on the positive side, the formation for tetragonal Zirconia proves that high temperature is attained in the combustion process.

All the synthesized samples are crystalline in nature with varying degrees of crystallinity within the same material and from material to material. XRD pattern of Zirconium gives the most intense peaks followed by Ceria and Lanthanum oxide.

The relative intensities of XRD peaks for Ceria and Zirconia match very closely with the standard patterns given in JCPDS data, except for one peak in Zirconia. This trend was not followed in case of Lanthanide oxide samples.

Ceria and Zirconia show better consistency compared to Lanthanum oxide. All samples of Ceria have been obtained in cubic form. Lanthanum oxide samples have three different hexagonal matches as per JCPDS files. Zirconia samples have tetragonal structures for high temperature combustion synthesis and monoclinic structure for relatively low temperature solid state synthesis. This is along reported lines.

The purpose of getting nanocrystalline material is served best in case of Ceria. This is analysed by comparing the standard unit cell volumes with the obtained ones.

In Ceria, shrinking of volume is observed in all samples in varying degrees. The shrinkage is maximum for the Ceria nanoparticle sample. On the basis of size reduction and surface effects, this can be said to be on expected lines. The red dots indicate the standard values obtained from JCPDS data while the black dots are for the observed values.

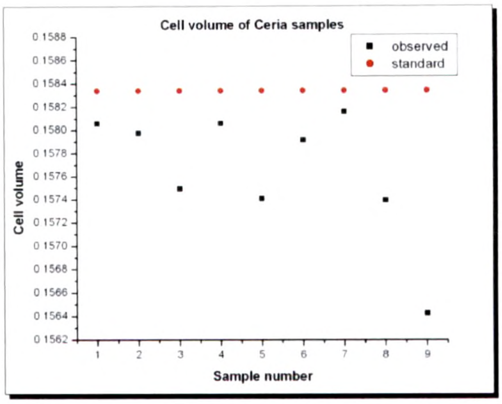

For the Lanthanum oxide samples, the comparison does not show consistency as in some samples the observed cell volumes is less while in others, it is more than the standard values. Result is almost consistent for two of the hexagonal phases, where shrinkage is seen. The third hexagonal phase shows an expanded cell, compared to the standard ones. The bigger dots are for standard values and the smaller for observed values. Zirconia samples also show the same kind of inconsistency for both monoclinic and tetragonal phases. Dots show standard values while stars show observed values.

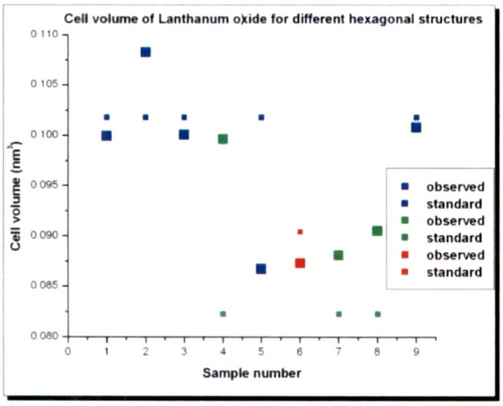

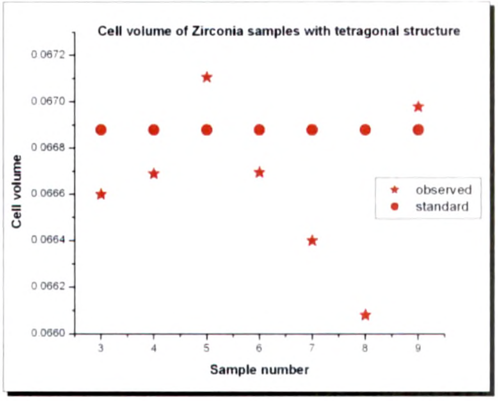

The crystallite and particle size was calculated first by the Scherer formula and then by graphical method. The graphical values are higher as the broadening of peaks due to strain is corrected in the process. No particular trend is seen. On average, the lowest crystallite/particle size was obtained in Ceria samples. Some degree of consistency in particle size was observed in the Lanthanide oxide samples and to a lesser degree in Ceria samples. Zirconia samples show wide variation.

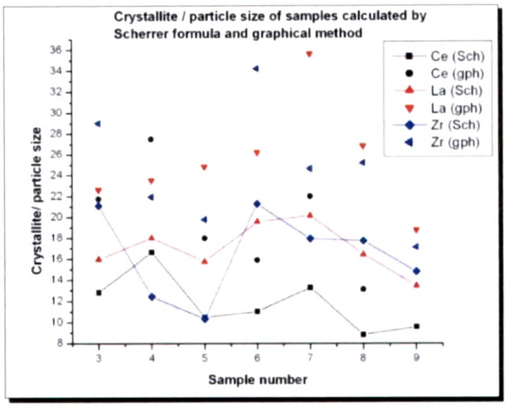

The lowest particle size was seen in case of nanoparticles of the three oxides prepared by co-precipitation method. Samples prepared in fuel lean proportions also gave relatively low crystallite size.

In Ceria and Lanthanum oxide, samples prepared in stoichiometric proportions have the highest crystallite size but for Zirconia, the maximum particle size is seen for samples with fuel rich proportions. The higher temperatures attained in stoichiometric and fuel rich ratio leads to aggregation and higher crystallite size.

The Scanning Electron Micrograph of samples prepared by solid state method show coarse hard particles in irregular shape with sharp edges. There is no porosity.

Combustion made samples have high porosity. The particles show non uniform growth with high agglomeration.

Co – precipitation samples have fine grains and are less agglomerated.

The porosity is very high in case of Ceria particles. Lanthanum oxide particles have foamy cotton like appearance. The Zirconia samples show chunks and rod like structures.

Co – precipitation made Zirconia sample has distinct spherical particles.

The fluorescence characteristics of Europium activated samples show variation for the different oxides and within the oxides for different synthesis techniques, both for emission as well as excitation.

Terbium activated samples are very consistent in their emission lines but have varying excitation spectra.

The oxide samples show good emission characteristics, except Terbium activated Ceria.

Europium activated Lanthanum oxide samples exhibit highest intensities of excitation and emission. The Zirconia samples have lower intensities and Ceria the lowest.

Terbium activated Zirconia samples have very high excitation and emission intensities compared to the Lanthanum oxide samples. The Ceria samples have very poor excitation and emission.

Amongst the bulk samples with Europium activation, the intensity is very high for Lanthanum oxide followed by Ceria and Zirconia.

Amongst the Europium activated Co – precipitation made samples too, Lanthanum oxide scores much higher compared to Zirconia. Intensity of Ceria sample is very low in comparison.

Average intensity of Furnace combustion made Europium activated samples is comparable in case of Lanthanum oxide and Zirconia but lower in case of Ceria.

Average intensity of microwave combustion made Europium activated samples is phenomenally high in Zirconia and comparatively much lower in the other two oxides.

Average intensities of furnace combustion made Terbium activated samples have phenomenally high intensities in Zirconia. For Lanthanum oxide, it is much less and for Ceria it is insignificant.

Average intensities of Microwave assisted combustion made Terbium activated samples again show phenomenal high intensities for Zirconia. Lanthanum oxide is on the lower side while Ceria is insignificant.

Zirconia shows better intensities in Terbium activated bulk sample, followed by lanthanum oxide.

Solid State and Co – precipitation methods show better results in Europium activated lanthanum oxide but combustion method gives better results in Zirconia.

Europium activated Ceria and Zirconia samples show a single predominant emission pattern, while Lanthanum oxide samples show two different kinds of emission patterns.

In Ceria, the 590 nm, ${}^5D_0 \rightarrow {}^7F_1$ magnetic dipole transition dominates over the higher wavelength ${}^5D_0 \rightarrow {}^7F_{2,3}$ electric dipole transitions. In Zirconia, electric dipole transitions

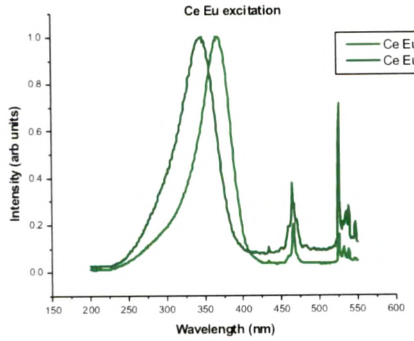

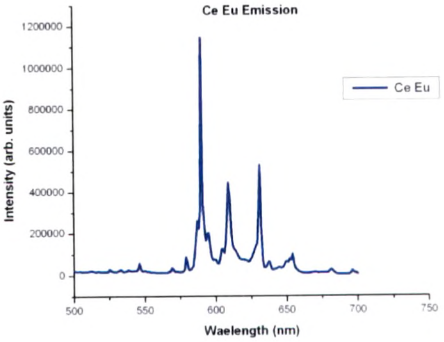

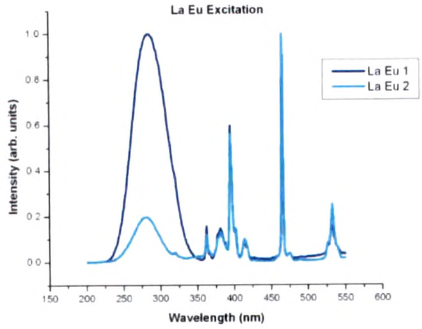

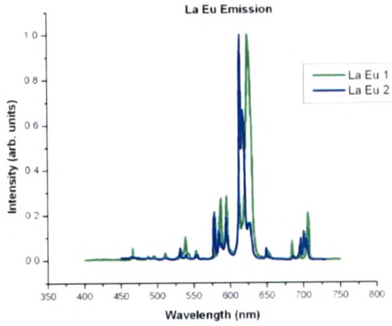

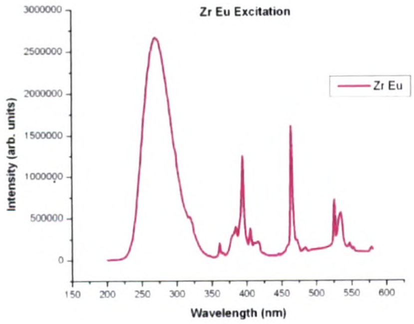

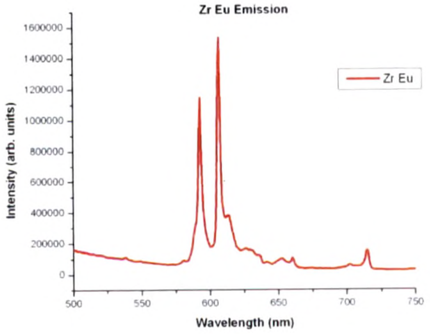

dominate over magnetic dipole transisions. In Lanthanum oxide the $^5D_0 \rightarrow {}^7F_1$ transitions are highly subdued. Samples exhibit two different emission trends with the higher emission intensity either at 614 nm or 624 nm. Excitation spectra of Europium activated samples have common features. There is a broad band attributed to the charge transfer transition and narrow bands of Eu^{3+} excitations. The broad band shifts on the account of the Eu – O bond lengths.

Terbium activated oxides have steady emission line at 545 nm. In Zirconia there is splitting of this emission peak.

Excitation spectra of Terbium activated samples show significant variations. Ceria remains insignificant while Lanthanum oxide has broad band as well as narrow band features. There is a shift in the peak wavelength of the broad band from samples to sample. This is assigned to the charge transfer band. Zirconia shows only host excitation for Terbium activation.

Pure Zirconia shows excitation as well as emission at 298 nm and 475 nm respectively. It is the only sample giving host emission with Eu^{3+} activation. Values of the ratio $^5D_0 \rightarrow {}^7F_2 / {}^5D_0 \rightarrow {}^7F_1$ show that the Ceria samples show least distortion, as the Eu^{3+} ions attain high inversion symmetry. The distribution of Eu^{3+} ions in Zirconia is in less orderly manner. Lanthanum is very poor in this aspect.

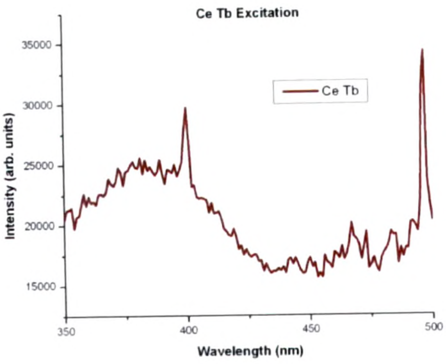
Ce Tb Excitation
Ce Tb
Intensity (arb. units)
35000
30000
25000
20000
15000
350
400
450
500
Wavelength (nm)

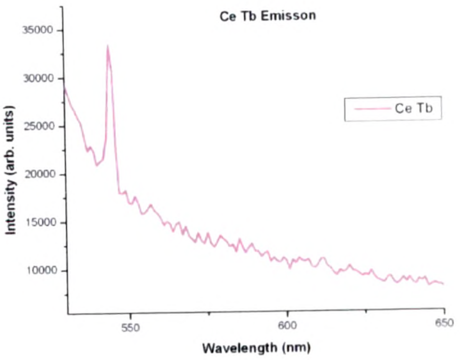
Ce Tb Emisson
Ce Tb
Intensity (arb. units)
35000
30000
25000
20000
15000
10000
550
600
650
Wavelength (nm)

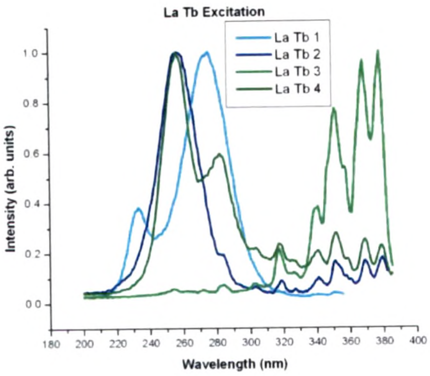
La Tb Excitation
La Tb 1
La Tb 2
La Tb 3
La Tb 4
Intensity (arb. units)
1.0
0.8
0.6
0.4
0.2
0.0
180
200
220
240
260
280
300
320
340
360
380
400
Wavelength (nm)

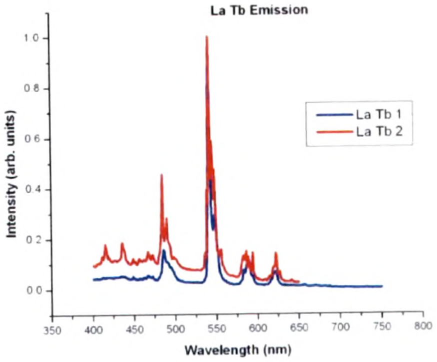
La Tb Emission
La Tb 1
La Tb 2
Intensity (arb. units)
1.0
0.8
0.6
0.4
0.2
0.0
350
400
450
500
550
600
650
700
750
800
Wavelength (nm)

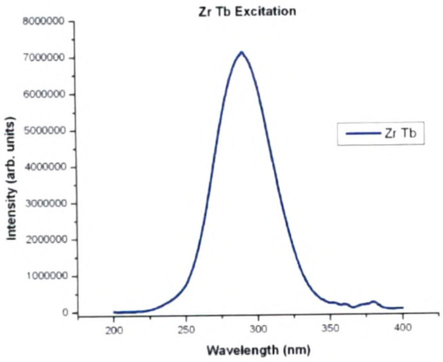
Zr Tb Excitation
Zr Tb
Intensity (arb. units)
8000000
7000000
6000000
5000000
4000000
3000000
2000000
1000000
0
200
250
300
350
400
Wavelength (nm)

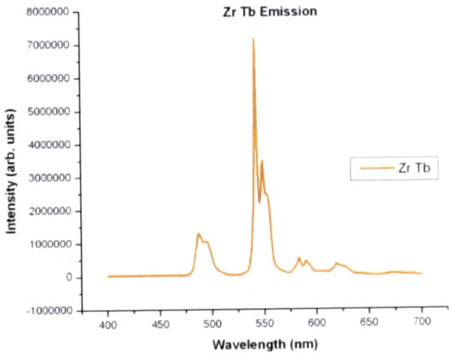
Zr Tb Emission
Zr Tb
Intensity (arb. units)
8000000
7000000
6000000
5000000
4000000
3000000
2000000
1000000
0
-1000000
400
450
500
550
600
650
700
Wavelength (nm)

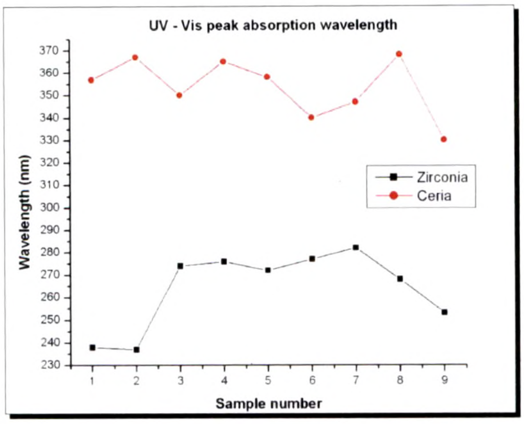

The UV visible peak absorption wavelengths for Zirconia are much lower than those of Ceria. Lanthanum oxide samples show flat UV- Visible characteristics.

The range of variation for peak absorption and peak excitation wavelengths is in conformity to each other.

7.2 Future Scope of Work

- Further studies are required to stabilize the combustion processes for consistent results and to understand the reasons for inconsistency.
- Attempts to alter the valence state of Europium from +3 to +2 by combustion synthesis needs to be taken up. Process with fuel lean ratio can be of use.
- Multiple activators can be incorporated to get emission at different regions of the visible spectrum in the same host.
- Surface passivation and capping of nanoparticles needs to be done to obtain better luminescence yield.
- Lanthanum oxide samples showing good emission properties need to be fine tuned in terms of synthesis techniques and parameters.
- Zirconia shows excellent potential as luminescent material. The system needs to be optimized.
- The potential of producing Zirconia on the mass scale using combustion method can be investigated.

JOURNAL OF RARE EARTHS
Vol.25, Spec. Issue, Dec. 2007, p.4

Synthesis and Characterization of Europium Doped Ceria *

Nishant. B. Shah, Biswajit. S. Chakrabarty*
(Applied Physics Department, Faculty of Technology & Engineering, M S University of Baroda, Vadodara, Gujarat 390001, India)

Abstract: Europium doped CeO_2 was synthesized via combustion synthesis method. The powders were found to be in a single phase. The average crystallite size was found to be about 30nm. It was revealed from photoluminescence spectra that there was an excitation band around 368 nm and a narrow excitation peak at 468 nm. The emission spectrum showed four peaks at 589, 608, 629 and 650 nm.

Key words: ceria; combustion synthesis; luminescence; excitation; emission; spectra; rare earths
CLC number: O614.33 **Document code:** A **Article ID:** 1002 - 0721(2007) - 0004 - 04

In recent years ceric oxide (CeO_2) powders have attracted a great deal of interest due to their unique properties and potential use in various industrial applications like catalyst for automotive exhaust gases, petroleum cracking catalyst, oxygen sensors, electrolytes for solid oxide fuel cells, UV absorbents and filters[1]. Due to its high refractive index, optical transparency, thermal and chemical stability and high dielectric constant, it also has potential applications in optical coating[2] and ion conduction layers[3,4].

There is a continuous search for new oxide phosphors as they possess very high chemical stability under electron excitation and in high vacuum. Sulphide phosphors are found to decompose during electron excitation and this leads to lower luminous efficiency[5]. Ceric oxide films have attracted attention as luminescent layers because of good compatibility with silicon based optoelectronics[6]. However less work is done on luminescence of CeO_2 powders doped with rare earth ions.

Tetravalent Cerium ion has no 4f electron. It can be a promising photoluminescent phosphor because of its strong light absorption characteristic through charge transfer from O^{2-} to Ce^{4+}. If energy is transmitted from this charge transfer state to rare earth ions, characteristic emissions are expected to be observed[6].

The combustion synthesis is a relatively simple and quick process with low cost and low energy consumption. The high temperature for the formation of the oxide phase directly from the precursor solution is achieved by the exothermicity of the gas phase redox reaction of combustible decomposition of products of metal nitrate-urea mixtures, releasing large amounts of gases like CO_2, N_2, and H_2O[7]. The term combustion refers to smoldering, flaming as well as explosive reaction. The volume of gases released lowers the temperature of the reaction and thus limits the contact among particles. So the synthesized powders have crystals generally in the nanometer scale and are more homogenous.

1 Experimental

1.1 Synthesis

Nitrates of metal and a fuel are taken in stoichometric ratio so that the heat released is maximum[8]. A.R. grade $Ce(NO_3)_3 \cdot 6H_2O$ (99.9% purity), $Eu(NO_3)_3 \cdot 6H_2O$ were taken as precursor material and Urea (NH_2-CO-NH_2) was taken as fuel. 2 percent Europium was added as a dopant. 5 ml water was added to make a solution. This solution was then transferred into a furnace kept at 600 ℃. The water quickly evaporated and the mixture boiled, frothed and auto ignited taking the shape of the container. Light yellow powders were produced. In case of solid state synthesis route Cerous nitrate was taken in a silica crucible and heated at 1000 ℃ for two hours. Off white colored powders were produced. Crystal structure, crystallite size and luminescence properties were investigated.

1.2 XRD Analysis

The powders were characterized using XRD.

• **Received date:** 2007 - 08 - 21; **revised date:** 2007 - 12 - 23
Biography: Nishant. B. Shah (1978 -), Male, Research scholar; Research field: Luminescence

* **Corresponding author** (E-mail: bschakrabarty@rediffmail.com)

XRD patterns were taken using a 40 kW, Shimadzu make LabX, X-ray diffractometer with Cu Kα radiation ($\lambda = 0.15418$ nm).

1.3 SEM analysis

The morphology of the $CeO_2:Eu^{3+}$ phosphor was observed using Shimadzu JEOL JSM-5610 LV electron microscopy instrument using accelerating voltages of 5 and 15 kV.

1.4 PL spectra

The excitation and emission spectra were taken at room temperature using Hitachi F 4500 series fluorescence spectrometer.

2 Results and Discussion

Figs. 1 & 2 show the XRD patterns for $CeO_2:Eu^{3+}$ phosphors made by Solid State and Combustion synthesis method respectively. The XRD peaks were indexed with those reported in the JCPDS card No.4-0593 confirming the formation of a single phase product. The *d* values corresponding to the three major peaks were found to be 0.313236 nm, 0.191609 nm and 0.163366 nm respectively. These values confirm the formation of pure fcc cubic fluorite type structure. There is a pronounced broadening of peaks in the combustion synthesized samples compared to their bulk forms as can be noticed from the Figures. The crystallite size was determined using the Debye Sherrer formula[9]. The average crystallite size was calculated and found to be about 30 nm for the sample prepared by combustion method.

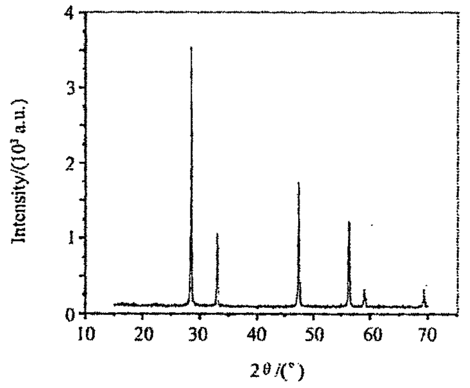

Fig.1 XRD patterns of $CeO_2:Eu^{3+}$ phosphor synthesized by solid state synthesis method

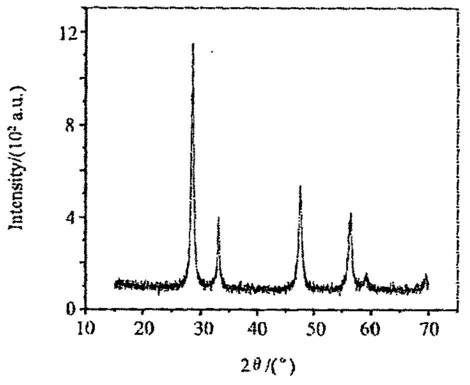

Fig.2 XRD patterns of as prepared $CeO_2:Eu^{3+}$ phosphor synthesized by combustion synthesis method

There is small shift in the peaks towards the lower side of 2θ values for the samples prepared by combustion method and corresponding increase in the lattice constant. This shift may be due to the larger surface area to volume ratio, which in turn increases the disorder of the nanostructure system.

SEM micrographs of combustion synthesized $CeO_2:Eu^{3+}$ phosphor are shown in Figs.3 and 4. The images show that the phosphor has high surface area. High amount of Porosity can be seen. Small particles agglomerate to form large size irregular shaped particles. The agglomeration may be due to high surface area. Both large and small particles are observed in Fig.3.

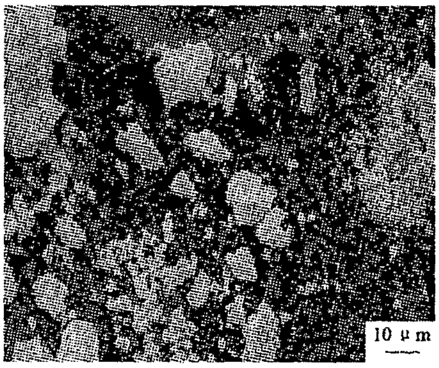

Fig.3 Scanning electron microscopy images of as prepared $CeO_2:Eu^{3+}$ phosphor synthesized by combustion synthesis method

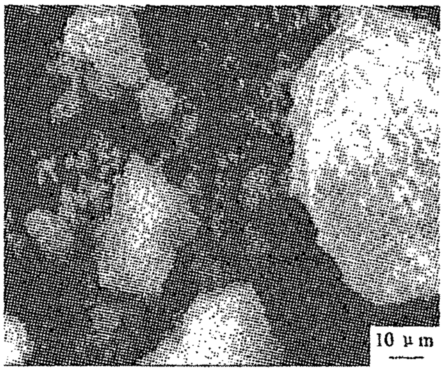

Fig.4 Scanning electron microscopy images of as prepared $CeO_2:Eu^{3+}$ phosphor synthesized by combustion synthesis method

The excitation spectra for the 589 and 608 nm emission lines as shown in Figs.5 and 6 consists of a broad band and a sharp peak. The broad Excitation band in the UV region peaking at 368 nm is attributed to the host CeO_2[10]. The energy absorbed by the charge transfer from O^{2-} to Ce^{4+} is transferred to Eu^{3+} ions producing red emission. The peak at 468 nm is assigned to direct excitation of Eu^{3+} ground state to higher levels of 4f manifold. It can be seen from the figure that the absorption at 368 nm is much stronger than at 468 nm. The excitation peak intensities for the 589 nm emission is much higher than for the 608 nm emission line. However, there is an increase in the intensity of 468 nm excitation relative to the 368 nm excitation in the latter.

The emission spectra were taken for an excitation wavelength of 368 and 468 nm for both the samples. Fig.7 shows the emission spectra of $CeO_2:Eu^{3+}$ excited at a wavelength of 368 nm. The multiple structured spectra consist of a series of well resolved features at 589, 608, 629 and 650 nm due to the splitting of the Eu^{3+} 4f shell. The peak at 589 nm has the highest intensity followed by the peaks at 608 and 629 nm. The dominant peak at 589 is due to the Eu^{3+} $^5D_0-^7F_1$ transition. The peaks at 629 and 608 nm are due to the $^5D_0-^7F_2$ transitions of Eu^{3+} ions[10]. The hump at 650 nm is due to $^5D_0-^7F_3$ transition.

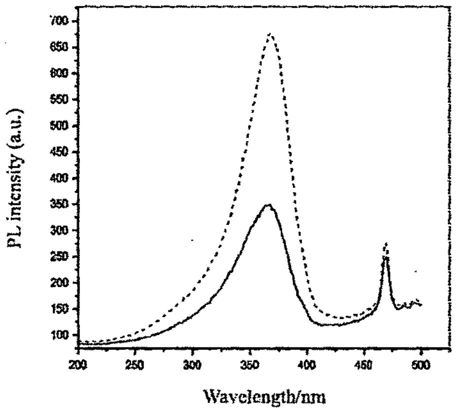

Fig.5 Excitation spectra for solid state (dotted line) and combustion (solid line) synthesized $CeO_2:Eu^{3+}$ crystals monitored at 589 nm

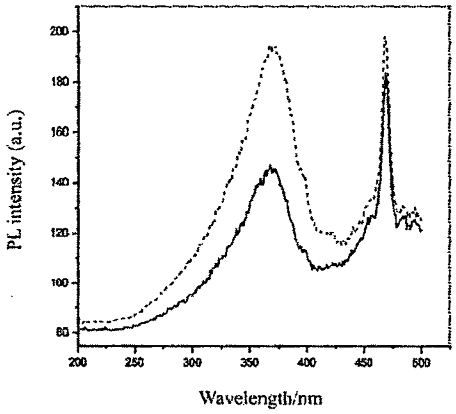

Fig.6 Excitation spectra for solid state (dotted line) and combustion (solid line) synthesized $CeO_2:Eu^{3+}$ crystals monitored at 608 nm

The $^5D_0-^7F_1$ is a magnetic dipole transition which scarcely changes with the crystal field around Eu^{3+} ion while the $^5D_0-^7F_2$ transition is electric dipole allowed and is hypersensitive to the crystal field around Eu^{3+} ions[11]. This transition tends to be more intense when Eu^{3+} ions are in a site with inversion symmetry. Therefore, the intensity ratio $^5D_0-^7F_2/^5D_0-^7F_1$ is a good measure of the rare earth ion site symmetry. From Fig.7 it can be observed that the symmetry ratio of Europium doped Ceria powders increases from bulk to nanosized powders. This result suggests that the symmetry of the sites occupied by Eu^{3+} ions increases from bulk to nanosized form in $CeO_2:Eu^{3+}$ phosphors. This leads us to conclude that the site of Eu^{3+} ion could have moved to the surface of the nanocrystal[11].

The emission spectra for 468 nm excitation is shown in Fig.8. Comparing with the Emission spectra for 368 nm excitation, it can be observed that the intensity of the 589 nm emission decreases sharply compared to 608 nm emission. This suggests that the energy transfer from CeO_2 host to Eu^{3+} ions, which gives 589 nm emission, dominates over intra 4f6 energy transfer.

It can be seen from the Figs.5 and 6 that the absorption in combustion synthesized phosphor is less compared to phosphor made by solid state synthesis

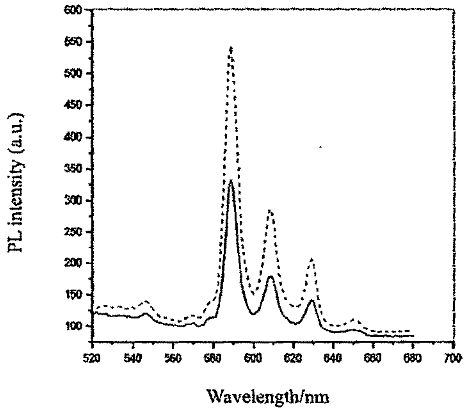

Fig.7 Emission spectra of solid state (dotted line) and combustion (solid line) synthesized $CeO_2:Eu^{3+}$ crystals at 368 nm excitation

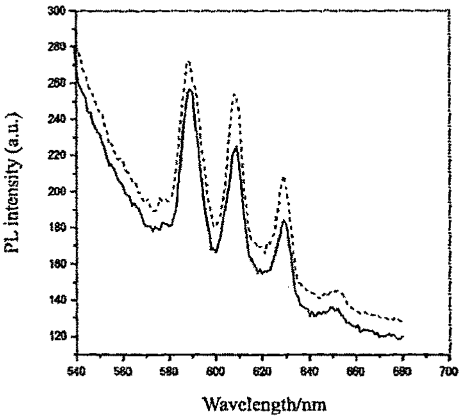

Fig.8 Emission spectra of solid state (dotted line) and combustion (solid line) synthesized $CeO_2:Eu^{3+}$ crystals at 468 nm excitation

method. It is also observed from Figs.7 and 8 that the luminescence intensity decreases in nanocrystals compared to their bulk form. This decrease may be due to surface and interface effects as they come into play when the Eu^{3+} ions move from bulk to the surface of the nanocrystals[11, 12].

3 Conclusion

Europium doped ceria was synthesized via Solid state and combustion synthesis routes. The XRD patterns showed the formation of a single phase product. Particle size by combustion synthesis was found to be 30 nm. The emission spectra recorded for the excitation of low pressure mercury i.e. 254 nm displayed similar peaks with very weak emission intensity.

From the fluorescence spectra it can be concluded that the emission at 368 nm excitation has highest intensity which is the resonance line of high pressure mercury. So this phosphor has a potential for application in High Pressure mercury vapour Lamps.

Acknowledgement: One of the authors N B Shah is thankful to the M S University of Baroda for providing University Research Scholarship.

References:

[1] Gu Lina, Meng Guangyao. *Mater Res. Bull.*, 2007 (Article In Press).

[2] Netterflelld R P, Sainty W G, Martin P J, Sie S H. *Appl Opt.*, 1985, **24**: 2267.

[3] Chen C C, Nasrallah M M, Anderson H U. *J. Electrochem. Soc.*, 1993, **140**: 3555.

[4] Punta E S, Stubenrauch J, Vohs J M, Gorte R J. *Langmuir*, 1995, **11**: 4832.

[5] Jiang Yongdong, Zhang Fuli, Summers Christopher J, Wang Zhonlin. *Appl. Phy. Lett.*, 1999, **74**: 1677.

[6] Shinobu Fujihara, Masashi Oikawa. *J. Appl. Physics*, 2004, **95**: 8002.

[7] Kingsley J J, Patil K C. *Materials Letters*, 1988, **6**: 427.

[8] Jain S R, Adiga K C, Verneker V R Rai. *Comb. Flame*, 1981, **40**: 71.

[9] C Suryanarayana, M Grant Norton. X-Ray Diffraction: A Practical approach, 1998 Plenum Press [M]. New York.

[10] Liu Xiaohua, Chen Shaojun, Wang Xiaodong. *J. Lumin*, (Article in Press).

[11] Wang R Y. *J. Lumin.*, 2004, **106**: 211.

[12] Tao Ye, Zhao Guiwen, Zhan Weiping, Xia Shangda. *Mater. Res. Bull.*, 1997, **32**: 501.